JACS
JOURNAL OF THE AMERICAN CHEMICAL SOCIETY
pubs.acs.org/JACS
Article

Ab Initio Molecular Dynamics of CdSe Quantum-Dot-Doped Glasses

Wenke Li, Xiujian Zhao, Chao Liu,* and François-Xavier Coudert*

Cite This: J. Am. Chem. Soc. 2020, 142, 3905−3912

ABSTRACT: We have probed the local atomic structure of the interface between a CdSe quantum dot (QD) and a sodium silicate glass matrix. Using ab initio molecular dynamics simulations, we determined the structural properties and bond lengths, in excellent agreement with previous experimental observations. On the basis of an analysis of radial distribution functions, coordination environment, and ring structures, we demonstrate that an important structural reconstruction occurs at the interface between the CdSe QD and the glass matrix. The incorporation of the CdSe QD disrupts the Na−O bonds, while stronger SiO_4 tetrahedra are reformed. The existence of the glass matrix breaks the stable 4-membered (4MR) and 6-membered (6MR) Cd−Se rings, and we observe a disassociated Cd atom migrated in the glass matrix. Besides, the formation of Se−Na and Cd−O linkages is observed at the CdSe QD/glass interface. These results significantly extend our understanding of the interfacial structure of CdSe QD-doped glasses and provide physical and chemical insight into the possible defect structure origin of CdSe QD, of interest to the fabrication of the highly luminescent CdSe QD-doped glasses.

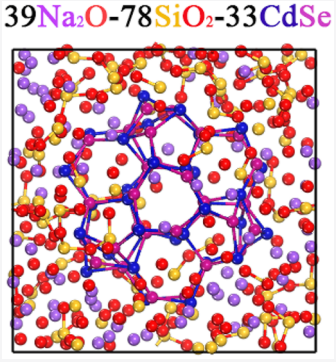

1. INTRODUCTION

The tunable optical and electronic properties of quantum dots induced by quantum confinement have stimulated enormous research interest. These properties were extensively explored for applications in the fields of lasers,[1] light-emitting diodes (LEDs),[2] and biolabeling.[3] Colloidal quantum dots exhibit excellent luminescence properties; however, the agglomeration of these QDs in solution severely restricts their practical applications. As an alternative, quantum-dot-doped glasses combine the good thermal and chemical stability of glass with easy access to device fabrication, hence offering potential applications in nonlinear optical devices[4] and LEDs.[5]

Quantum dots were first fabricated in a glass matrix by Ekimov et al. in 1981.[6] Brus[7] et al. first synthesized quantum dots in colloidal solutions in 1983. The past few decades have witnessed the blossoming of research in quantum dots, and chemically fabricated quantum dots can exhibit a high photoluminescence quantum yield (PLQY) after surface passivation. Compared to their colloidal counterparts, quantum dots embedded in a glass matrix display poor PLQY, and the highest PLQYs for CdSe embedded in glass have been measured at 3%[8] until now. The enormous difference in the PLQY between QDs in colloidal solutions and in glass matrixes naturally leads to the following question: why is the quantum efficiency in the glass matrix so low? How can this situation be improved to promote the practical applications of quantum dots? Experimentalists have worked for decades to shed light on these issues, and some mechanisms have been established to explain this phenomenon. It has been assumed that the presence of defects at the interface between QD and the glass matrix can quench the excitonic emission and produce unfavorable defect emission, which is detrimental to applications.[9] However, it is experimentally challenging to probe the origins of the interfacial defects and to characterize the structure and chemical environment of CdSe quantum-dot-doped glass because of the inadequate resolution of the existing techniques, the instability of the glass matrix under an electronic beam, and the relatively low concentration of QDs in the glass.

Theoretical modeling has been applied as an alternative to bring insight into these issues, and a comprehensive exploration of the local atomic structure can give guidance on the design of highly luminescent glasses. Computational materials studies have become very popular due to increasing computational power and the development of efficient numerical algorithms and can investigate a system at the atomistic level, which is not directly possible in experiments, gaining insight into both physical and chemical properties of materials. The two main computational methods for materials are classical approaches and ab initio simulations. Both classical molecular dynamics (MD) and ab initio molecular dynamics (AIMD) have been successfully used in modeling various multicomponent glass materials[10−16] and CdSe nanocrystals.[17−23] However, in spite of these extensive theoretical studies for these two separate systems, no atomistic

Received: November 8, 2019
Published: February 3, 2020

https://dx.doi.org/10.1021/jacs.9b12073
J. Am. Chem. Soc. 2020, 142, 3905−3912

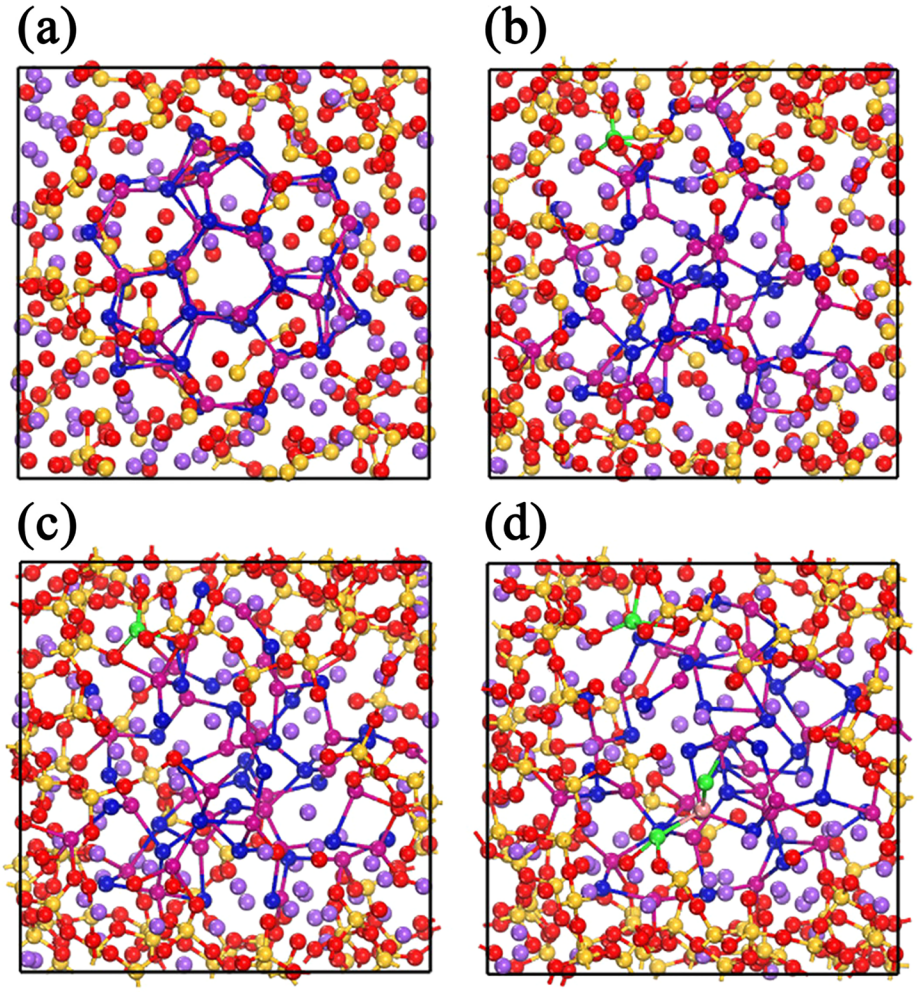

Figure 1. (a) Initial configuration for the classical MD calculations. (b) Final configuration for classical MD simulations, used as the initial configuration for the geometry optimization by the DFT method. (c) Geometry-optimized structure at the DFT level, used as the initial configuration for the ab initio molecular dynamics. (d) Final configuration from the AIMD simulations. Si, yellow; O, red; Na, purple; Se, magenta; Cd, blue. Se and Cd atoms dissociated from the quantum dot are highlighted in pink and green, respectively.

calculations have been conducted so far on the composite QD/glass systems and their interfacial properties.

In this work, we have employed ab initio molecular dynamics in order to model CdSe QD embedded in a glass matrix, with a particular focus on the reconstruction occurring at the QD/glass interface. We started from classical MD calculations of the glass matrix and quantum chemical models of the quantum dots. Because the interaction between the CdSe QD and glass matrix cannot be described accurately in classical MD due to the lack of the appropriate interatomic potentials, we used ab initio methods. Our ab initio MD methodology is based on quantum mechanics at the density functional theory (DFT) level, which means it does not rely on a fixed functional form for interatomic interactions, but the electronic degrees of freedom of each atom are fully modeled. Due to the limitation of computational power cost, we chose a model of the composite system with the composition of $60Na_2O$-$120SiO_2$-33CdSe to conduct the AIMD simulations. The radial distribution functions for Si−O, Na−O, Cd−Se, Cd−O, Se−O, Se−Na, Se−Se, and Cd−Cd were calculated to compare with experimental counterparts. The coordination environment and the ring structures were analyzed. The results demonstrate that enormous structural reconstruction happens simultaneously in QD and the glass matrix, with the creation of Cd−O bonds and Se−Na bonds at the interface. The incorporation of the CdSe QD disrupts Na−O bonds, while stronger SiO_4 tetrahedra are reformed. The glass matrix contributes to great structural reconstruction at the external surface of the quantum dot, making it hard to maintain the bulk structure even at its core. The results reported here can give a better fundamental understanding of this complex system and give insight into the fabrication of highly luminescent glasses containing quantum dots.

2. COMPUTATIONAL METHODS

2.1. Generation of a Glass Matrix Structure. The starting configuration for the glass matrix was generated by placing atoms randomly in a cubic simulation box. The total number of atoms for the glass was 540 (120 Na, 120 Si, and 300 O), with the simulation cell sizes ($a = b = c = 19.383$ Å, $\alpha = \beta = \gamma = 90°$) kept constant throughout the simulation, giving a density consistent with experimental values ($\rho = 2.492$ g/cm^3).[15] Hard constraints were imposed to avoid unphysically small interatomic distances. An initial classical molecular dynamics simulation was performed using a partial-charge rigid-ion pairwise potential developed by Pedone et al.,[16] with the DL_POLY classic package.[24] The Coulomb interactions were calculated using the Ewald summation method[25] with a precision of 10^{-5} and a real-space cutoff for short-range interactions set to 7.6 Å. The Verlet algorithm was applied for the integration of the equations

https://dx.doi.org/10.1021/jacs.9b12073
J. Am. Chem. Soc. 2020, 142, 3905−3912

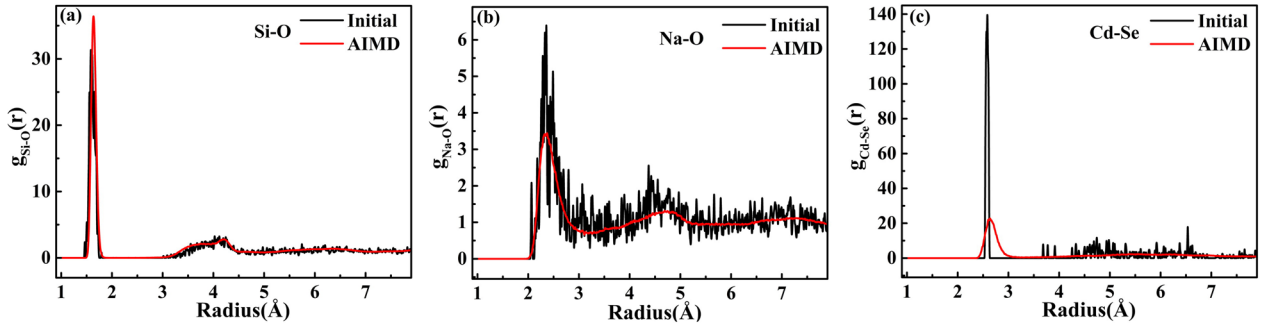

Figure 2. Radial distribution functions for (a) Si−O, (b) Na−O, and (c) Cd−Se pairs in the initial structure (black) and averaged over the ab initio molecular dynamics (red) for a quantum dot embedded in the glass matrix.

of motion with a time step of 1 fs. The glass structures were generated using a melt-quenching approach in the NVT ensemble at the target density from experimental data, using a Nosé−Hoover thermostat[26−28] with a relaxation time of 0.1 ps. The initial structure was heated up gradually in steps of 1000 K with a 60 ps MD run at each temperature from 300 to 6000 K. After equilibration of the liquid at 6000 K during 400 ps, the system was cooled gradually in steps of 500 K with a 60 ps MD run at each temperature from 6000 to 300 K. Another 200 ps NVT simulation was carried out at 300 K, together with a 200 ps NVE simulation in order to equilibrate the structure.

2.2. Generation of the CdSe Quantum-Dot-Doped Glass Structure. The experimental mechanism for the formation of CdSe QDs in glass is based on the phase decomposition of oversaturated solid solution,[9] and the time scale of the growth of these nanocrystals is far beyond the current computational method. Therefore, it is difficult to simulate the nucleation and growth stages, and here we directly introduced the CdSe QD into the glass matrix rather than trying to model directly the melt-quenching process. The $Cd_{33}Se_{33}$ QD (with a diameter of 13 Å) obtained in our previous work[29] was incorporated into the glass matrix, removing glass atoms so interatomic distances between the QD and the glass matrix were longer than 2.5 Å. The final composition was 39 Na_2O−78 SiO_2−33 CdSe (Figure 1a). The interatomic interactions in CdSe QD used a Lenard-Jones pairwise potential validated in the literature[22,23] and the Lorentz−Berthelot combining rules were used for interactions between CdSe QD and the glass matrix. The whole structure was equilibrated at 1000 K, first using 200 ps of NVT dynamics and then 200 ps of NVE dynamics, initially with atoms frozen from the CdSe QD. The structure was then cooled gradually in steps of 50 K with a 60 ps MD run at each temperature from 1000 to 500 K while keeping CdSe QD frozen. Subsequent cooling from 500 to 300 K took place in steps of 10 K, with all atoms allowed to move. Finally, the structures were further equilibrated at 300 K with 200 ps NVT dynamics and final 200 ps NVE dynamics (Figure 1b). This simulation methodology was followed after comparison with several other simulations in order to allow full relaxation of the system (especially the glass at high temperature) while maintaining the integrity of the quantum dot. We have explored several quenching methods of the whole structures, and the size of the glass matrix has been altered to test the representation of our current model, which can be found in the Supporting Information.

2.3. Ab Initio Molecular Dynamics of a CdSe Quantum Dot in a Glass Matrix. After the equilibration of systems using the classical MD simulations described above, we used the resulting configurations as a starting point for ab initio modeling at the density functional theory (DFT) level, using the Kohn−Sham formulation as implemented in the CP2K code.[30] Simulations were run at the generalized gradient approximation level, employing the PBE exchange−correlation functional.[31] The plane wave cutoff was set to 600 Ry. For Na, Cd, and Se, we used short-range molecularly optimized double-ζ single polarized basis sets (DZVP-MOLOPT-SR-GTH), while for O and Si we used a double-ζ single polarized basis set (DZVP-MOLOPT-GTH).[32,33] After an initial geometry optimization with DFT, the resulting relaxed structure (Figure 1c) was used as the initial structure for the AIMD simulations. The structure was quenched from 500 to 300 K in steps of 50 K, with a total 10 ps AIMD run at a time step of 2 fs. The production run was conducted in the NVT ensemble at 300 K for 10 ps.

3. RESULTS AND DISCUSSION

Our goal in this work is to analyze the nature of the QD/glass matrix interface and to quantify the reconstruction that takes place. As such, our initial structure (Figure 1a) is a "naïve" view of the hybrid system and is somewhat representative of the simplistic models that are sometimes used in the existing literature. By visual inspection, large structural reconstructions occurred after equilibration of the system, regardless of whether it is the final configuration of classical MD simulations of the glass matrix relaxation (Figure 1b), the DFT geometry optimization (Figure 1c), or the final structure of AIMD simulations (Figure 1d). In particular, we clearly observed the influence of the matrix in the introduction of strong disorder in the quantum dot. For the original QD structure, the Cd atoms were either coordinated with four Se atoms (in the core of the QD) or three Se atoms (on its external surface). A more complex coordination of the Cd and Se atoms in the glass-embedded QD can be observed, where some of the Cd−Se linkages were broken, the coordination rings were opened, and the coordination between the QD and glass was observed. The QD, in its glass matrix, cannot maintain its pristine structure, which was different from most of the models studied in the existing literature of QD in solution.[17,19]

In addition to these changes in the environment of the QD atoms, we observed some Cd ions from the QD surface that completely dissociated from the quantum dot structure and migrated into the glass matrix (highlighted in green in Figure 1). This was observed for one atom during MD at the classical level and confirmed in the AIMD with the migration of a second ion. Furthermore, during the ab initio MD we observed the dissociation of Cd−Se−Cd clusters (with the Se atom highlighted in pink). For the system size under study here, the percentages of dissociation were found to be 1.52% (Figure 1b,c) and 6.06% (Figure 1d), respectively. These observations on the microscopic scale were novel and were in good agreement with the experimental evidence of Cd atoms found to be dissolved in the matrix in as-prepared glass, seen by the extended X-ray absorption fine structure spectroscopy analysis (EXAFS),[34] in the CdSe QD-doped glass with the initial composition of 50 SiO_2−20 K_2O−20 ZnO−5 B_2O_3−1.5 CdO−1.5 CdS−1.0 Na_2SeO_3(wt %), the Cd−O contacts in all specimens with different thermal treatment were observed, attributed to the cadmium dissolved in the glass matrix.

https://dx.doi.org/10.1021/jacs.9b12073
J. Am. Chem. Soc. 2020, 142, 3905−3912

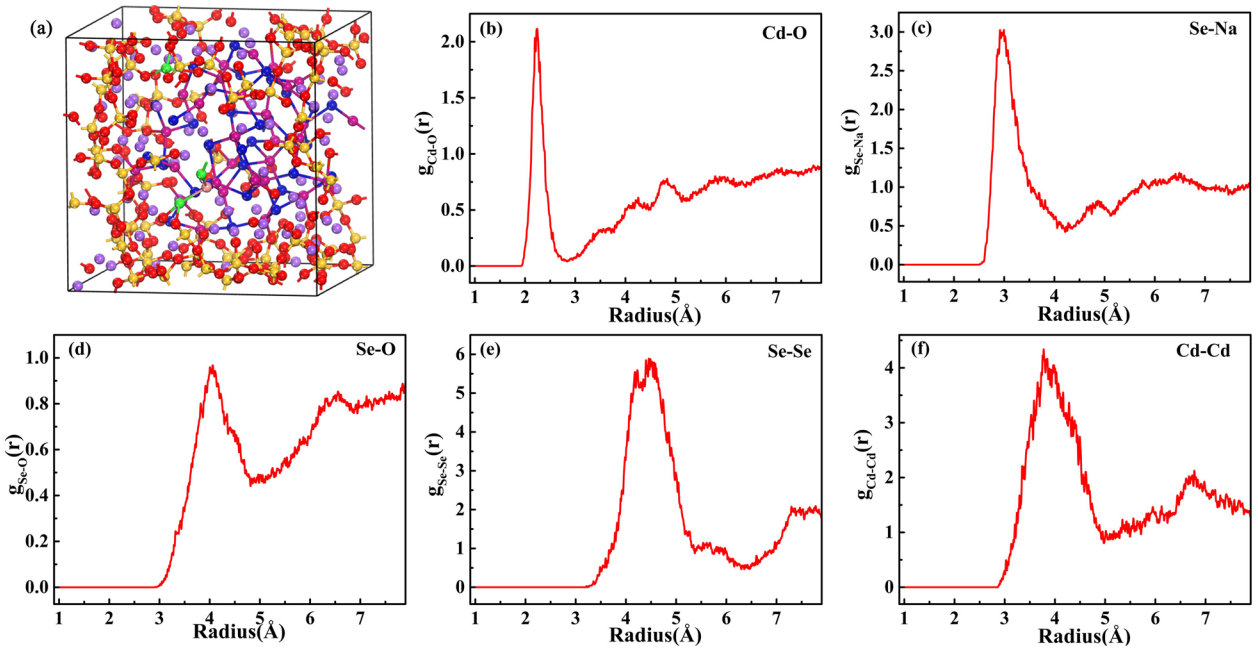

Figure 3. (a) Final configuration from the ab initio molecular dynamics. Radial distribution functions for (b) Cd−O, (c) Se−Na, (d) Se−O, (e) Se−Se, and (f) Cd−Cd pairs, averaged over the ab initio molecular dynamics (red), for a quantum dot embedded in the glass matrix.

Table 1. Average Coordination Number and Percentages of Na, O, Si, Se, and Cd with Different Atoms in the Initial Configuration and Averaged over the Ab Initio MD Simulation

system		initial structure		ab initio MD	
atom	bond	coordination number	percentages	coordination number	percentages
Na	Na−O	4.06	88.80	3.54	86.21
	Na−Se	0.08	1.68	0.33	8.05
O	O−Na	1.63	52.40	1.42	44.54
	O−Si	1.42	45.62	1.60	50.29
	O−Cd			0.16	5.17
Si	Si−O	3.54	87.64	4.00	100
Se	Se−Cd	3.36	82.84	2.52	76.26
	Se−Na	0.18	4.48	0.78	23.72
	Se−O	0.36	8.96		
Cd	Cd−O			0.97	27.70
	Cd−Se	3.36	94.87	2.52	71.72

We then analyzed the radial distribution functions for Si−O (Figure 2a), Na−O (Figure 2b), and Cd−Se (Figure 2c) pairs. In each case, we compared RDFs for the initial structure (Figure 1a) and distribution functions obtained over the ab initio molecular dynamics simulation. Compared with the initial structure, only minor changes in Si−O and Na−O interatomic distances were observed, with first-neighbor peaks at 1.64 and 2.34 Å, respectively, consistent with the experimental value.[13,14]

Interestingly, an evolution in the Cd−Se distances was observed, from 2.59 Å to a broader distribution with an average of 2.64 Å (2% longer), due to both the finite temperature and the influence of the glass matrix, which weakens some of the Cd−Se bonds. This influence of coordination was previously discussed in the literature.[21,35−39] The Cd−Se bond length was 2.68 Å when one Se atom was coordinated with four Cd atoms and 2.62 Å when one Se atom was coordinated with three Cd atoms in $Cd_{33}Se_{33}$ clusters.[20] In this context, it was also interesting to note the size dependence of the Cd−Se bond length, i.e., the smaller the QD's size, the shorter the Cd−Se bond length,[38,39] while a lattice contraction was observed in the CdSe QD-doped glasses.[40] This effect was linked to the surface/volume ratio, where smaller QDs had more surface atoms with shorted Cd−Se bonds. We noted however in our ab initio MD simulations that the diameter of the QD in the final structure was 16 Å, which increased from 13 Å in the initial structure. This demonstrates that the glass-embedded QD does not behave like the QD in vacuum: first, because of the chemical environment that the glass matrix constitutes, with glass/QD coordination. But other explanations have been advanced in the literature, and it was suggested that the isotropic nature of the ordering of QDs in solution[41] gives rise to the strain effects between QDs and solution, resulting in the size-dependent and ligand-dependent reconstruction of the QD surface. Moreover, the thermal and elastic mismatch between the nanocrystals and glass matrix can give rise to residual stresses upon cooling,[42−44] increasing the extent of surface reconstruction.

We now turn our attention to the QD/glass interface (Figure 3a). Looking at the respective radial distribution

https://dx.doi.org/10.1021/jacs.9b12073
J. Am. Chem. Soc. 2020, 142, 3905−3912

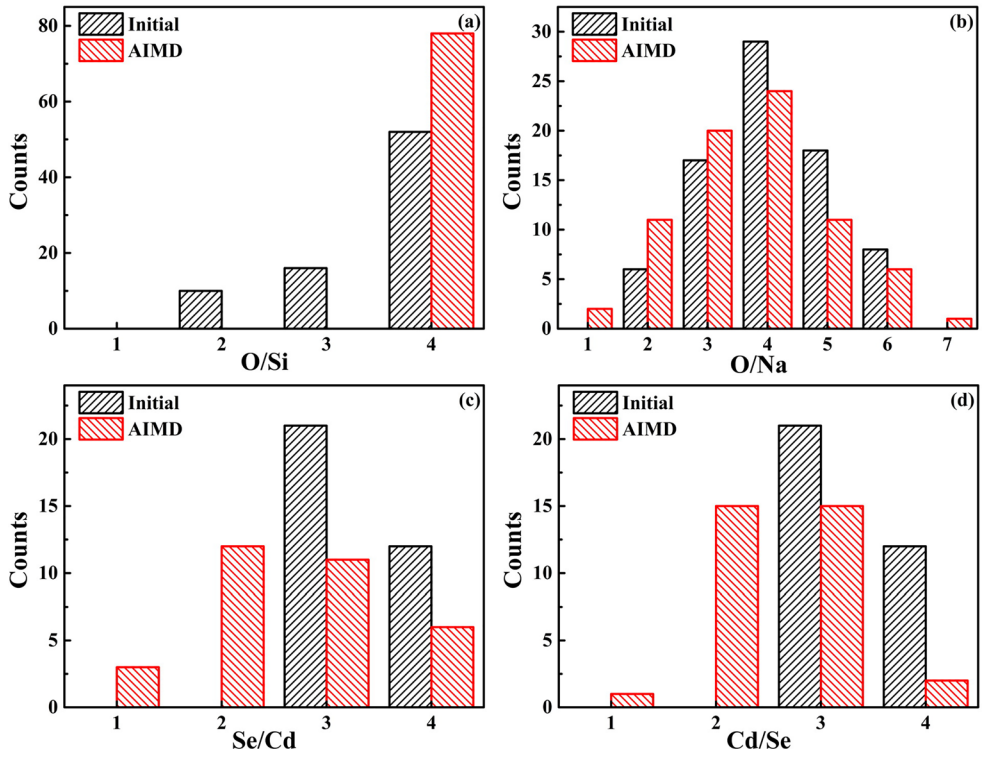

Figure 4. Histograms of coordination numbers for different pairs of atoms, comparing the initial structure (in black) and the average over the ab initio MD simulation (in red). (a) O coordination around Si atoms. (b) O coordination around Na atoms. (c) Se coordination around Cd atoms. (d) Cd coordination around Se atoms.

functions, we observed the formation of Cd−O and Se−Na bonds. They were characterized by interatomic distances of 2.25 Å (Figure 3b) and 2.91 Å (Figure 3c), respectively. These values, obtained from the ab initio molecular dynamics, were in excellent agreement with the experimental data available. The interatomic Cd−O distances were found to be 2.25 Å based on the EXAFS characterization of CdSe QD-doped glasses,[34] while the Se−Na distance in the bulk Na_2Se structure was 2.95 Å (Crystallography Open Database ID: 9009065). From the experimental crystal lattice energies of CdO, CdSe, Na_2O and Na_2Se,[45] we expect the Na−Se bond to be weaker than the Na−O bond and the Cd−O bond to be stronger than the Cd−Se bond. This can explain that the driving force for this reconstruction has its roots in the Cd−O interactions. On the other hand, ab initio MD simulations confirm that there were no close contacts with the formation of Se−O (Figure 3d), Se−Se (Figure 3e), and Cd−Cd pairs (Figure 3f) at the QD/glass interface. The interatomic distances of these bonds were 3.92, 4.46, and 3.70 Å, inconsistent with the experimental values, which were 1.83,[29] 2.53,[34] and 4.20 Å.[34]

In order to understand the QD/glass interface in depth, the coordination environment (Table 1) as well as the ring structures inside the CdSe QD/glass systems were explored. We found that 52.40% of O atoms were bonded to Na atoms in the initial structure, while in the ab initio MD that number was 44.54%. Meanwhile, there were opposite tendencies for the coordination between O and Si atoms, with the percentages increased from 45.62% (initial structure) to 50.29% (ab initio MD). Moreover, while there was no Cd−O bond in the initial structure, the AIMD showed that 5.17% of O atoms were bonded with Cd atoms, confirming the formation of Cd−O bonds in the interface.

Somewhat surprisingly, 100% of Si atoms were 4-coordinate with O atoms, while the coordination number of the Si atom with O atoms was 3.54 in the initial structure. This points to a dissymmetry in the Si−O and Na−O bonds of the glass, where the presence of the QD leads to the disruption of the Na−O bonds, while Si−O coordination (and Cd−O, to a smaller extent) is kept intact due to its stronger bond. In addition, the glass matrix also has a marked impact on the Cd−Se bonds in the QD. Se atoms (23.72%) were bonded with Na atoms and Cd atoms (27.70%) were bonded with O atoms in the QD/glass interface, with a great decrease in the number of bonds between Cd and Se atoms.

It should be noted here that in our previous work[29] we studied a simple model of $Cd_{33}Se_{33}$ clusters capped with one sodium ion and demonstrated that this results in the introduction of defect states in the HOMO−LUMO gap, giving rise to unusual near-infrared luminescence. In addition, the HOMO and LUMO states were spread in the same region, indicating the high probability of recombination of holes and electrons excited from these defect states. The results obtained in this work from ab initio MD show that when QD is surrounded by a glass matrix the number of surrounding sodium ions within a short distance (Na−Se linkages) is quite important. The defects at the interface are found not to be as simple as we expected in our previous work: a large percentage of Se atoms are bonded with Na atoms in our glass, where Na_2O was introduced as a glass modifier. The abundant nature of the sodium atoms in the glass matrix will greatly contribute to the defect emission, and a decrease in sodium content may diminish the number of interfacial defects, giving guidance to the design of the glass composition in future work.

We further analyzed the details of the coordination numbers for Si−O pairs (Figure 4a), Na−O pairs (Figure 4b), Cd−Se

https://dx.doi.org/10.1021/jacs.9b12073
J. Am. Chem. Soc. 2020, 142, 3905−3912

pairs (Figure 4c), and Se−Cd pairs (Figure 4d). These confirmed the strong rearrangement of the interface to promote the formation of SiO_4 tetrahedra, which was also seen in the ring statistics (Table 2) along with the occurrence of small ring sizes for Si−O rings. For example, we observed 16 8-membered rings (8MR) in the final structure, while no such ring was present in the initial configuration. Consistent with the data in Table 1, the occurrence of higher coordination numbers of Na atoms with O atoms (O/Na = 6, 5, and 4) decreased while the frequency of lower coordination number for Na atoms with O atoms increased (O/Na = 3, 2, 1) compared with the initial structure (Figure 4b). Additionally, we observed a clear reduction of Na−O rings for all ring sizes but especially for the 4-membered rings. This strengthened our conclusion that the rearrangement at the interface of the CdSe QD causes Na−O bonds to maintain their Si−O coordination.

Table 2. Number of Rings of Different Sizes for Different Ring Members in Initial Structures and Averaged over Ab Initio Molecular Dynamics

ring members	ring size	initial structure	ab initio MD
Si−O	8		16
	10	3	10
	12		4
	14	1	1
	16	1	
Na−O	4	88	45
	6	26	9
	8	16	2
Cd−Se	4	12	1
	6	67	3
	8	6	7
	10		4
	12		1

The basic coordination environments of the CdSe QDs are $CdSe_4$ and $CdSe_3$, whose counts were 12 and 21 in the initial structure, respectively. However, the average number of Se atoms around Cd decreased, with counts for $CdSe_4$, $CdSe_3$, $CdSe_2$, and $CdSe_1$ of 6, 11, 12, and 3 in the ab initio MD (Figure 4c), respectively. The total number of Cd atoms bonded with Se atoms was 32, with 1 Cd atom not bonded to any Se atom (migrated in the glass matrix, see Figure 1d). In terms of the coordination environment of Se atoms, all of the Se atoms were bonded with Cd atoms in the initial and final structures. The number of Se atoms with Cd/Se ratios of 4 and 3 changed from 12 and 21 to 2 and 15, respectively. At the same time, the appearance of the Se atoms with Cd/Se = 2 and 1 was observed (Figure 4d). The obvious changes in the ring size of Cd−Se member rings confirmed the huge reconstruction of the quantum dot. The 4- and 6--membered Cd−Se rings opened up, with only one 4-membered and three 6-membered Cd−Se rings left in the final structure. The significant reconstruction of QD in this work distinguishes it from other work for the reason that the QDs almost keep the bulk structure in the center in other computer simulations. The common method of exploring the QDs in solutions was to passivate the surface atom with a limited number of organic ligands while the QD was incorporated into the inorganic glass matrix in our work. Only the surface atoms were capped with organic ligands, without the simulation of the real chemical environment of the solution, leading to the smaller structural reconstruction compared to our work. Although there were some simulations in which the QD was directly introduced into the solid matrix,[46] our work was aimed at the amorphous inorganic matrix for the first time, which constitutes a large part of the research regarding the application of QDs for which the atomic structure and origin of defect emission have been rarely studied. The simulations in our work are closer to the real situation of a QD in a glass matrix, in which the matrix can have a more direct influence on the QD compared with the intended passivation of the QD.[17,19,20] Apart from the different initial structure building method, the difference in the bond nature between the inorganic atoms with QDs, such as glass modifiers Na atoms and nonbridging O atoms, and the organic ligand with QDs might have a relation to the different structures of QDs in the glass matrix and solutions.

4. CONCLUSIONS AND PERSPECTIVES

To the best of our knowledge, our calculations are the first ab initio molecular dynamics study of a CdSe quantum dot embedded in a glass matrix. In particular, the structure of the CdSe QD-doped glass was obtained by the melt-quenching method, generated by the combination of the molecular dynamics and the ab initio molecular dynamics. Distinct structural reconstructions were observed simultaneously in the glass matrix and CdSe QD. The incorporation of CdSe QD greatly disrupts the bonds between Na atoms and O atoms, with the reduction in the number of O atoms bonded with Na atoms replaced by the Si atoms and Cd atoms. Unexpectedly, it also gives rise to the formation of the SiO_4 tetrahedra and the small ring size of Si−O member rings, with all of the Si atoms being 4-coordinate with the O atoms in the final structure. As for the interfacial structure, both the radial distribution function for the interatomic distance of Cd atoms and O atoms, Se atoms, and Na atoms as well as the analysis of the coordination environment of these atoms directly confirm the existence of the Cd−O bonds and Se−Na bonds, consistent with the experimental findings. Furthermore, it seems like there is little possibility of the formation of the Se−O bonds, Se−Se bonds, and Cd−Cd bonds. In terms of the CdSe QD, the glass matrix has a greater influence on the reconstruction of the QD compared to QD in solution. It is hard to maintain the stable 3- and 4-coordinate CdSe basic units when they are introduced into the glass matrix, with the 3- and 4-membered rings disappearing. Additionally, the disassociated Cd atoms and Se−Cd−Se clusters were observed to be migrated in the glass matrix. The complex structure of the glass matrix and the difference in the bond nature between the inorganic ions and QD might be attributed to the instability of QD in the glass matrix compared with the QD in organic solutions.

Our work gives an intuitive visual illustration of the local atomic interfacial structure of the CdSe QD-doped glass, promoting our understanding of the structural reconstructions of the glass matrix as well as the CdSe QD. Our results shed light on the impacts of the glass matrix on the CdSe QD, exploring the possible defect structure of the QD and thus giving guidance for the adjustment of the component of the glass matrix and for the fabrication of highly luminescent CdSe QD-doped glasses. Our work suggests that it is worth adjusting the amount of sodium in the glass composition, which greatly contributes to the trap states in the band gap and leads to unfavorable defect emission. At the same time, we recommend reaching a compromise between the low sodium contents and melting temperature because sodium can largely alter the

https://dx.doi.org/10.1021/jacs.9b12073
J. Am. Chem. Soc. 2020, 142, 3905−3912

melting point of glass. Besides, our results demonstrated that the surface Cd atoms are more likely to be passivated by the oxygen in the glass matrix, which may provide the possibility of fabricating core−shell CdSe QDs by adjusting the thermal treatment. The fabrication of a core−shell structure of CdSe QDs is more difficult and less explored compared with colloidal quantum dots. Work is in progress to extend our understanding of the electronic structure of these hybrid systems.

In our future work, various glass systems will be studied and we will explore the possible thermal strategies for synthesizing core−shell CdSe quantum dots according to the insight gained from ab initio molecular dynamics. We also aim at studying more in depth the influence of the QD size on the nature of the QD/glass interface and the properties of the hybrid system. While the influence of QD size on its emission properties is well-known for QDs in solution, the nature of the interface reconstruction for QDs embedded in glass matrixes is not currently known. We expect, from the results obtained in this work, that the interfacial reconstruction remains similar: it is, after all, linked in large part not to the system size but to the nature of the competition among Cd−Se, Cd−O, and Na−O interactions. However, because the surface/bulk ratio is directly linked to the size of the QD, the properties of the composite systems would be affected. While it is not currently possible to explore larger QD sizes at the level of theory chosen here (ab initio molecular dynamics), studies using QM/MM strategies could be of use in order to directly address the question of larger quantum dot sizes.

■ ASSOCIATED CONTENT

Supporting Information

The Supporting Information is available free of charge at https://pubs.acs.org/doi/10.1021/jacs.9b12073.

Computational details of different quenching methods, computational details on different system sizes, and additional discussion (PDF)

CIF files (ZIP)

■ AUTHOR INFORMATION

Corresponding Authors

Chao Liu − *State Key Laboratory of Silicate Materials for Architectures, Wuhan University of Technology, Hubei 430070, China;* orcid.org/0000-0003-4324-6409; Email: hite@whut.edu.cn

François-Xavier Coudert − *Chimie ParisTech, PSL University, CNRS, Institut de Recherche de Chimie Paris, 75005 Paris, France;* orcid.org/0000-0001-5318-3910; Email: fx.coudert@chimieparistech.psl.eu

Authors

Wenke Li − *State Key Laboratory of Silicate Materials for Architectures, Wuhan University of Technology, Hubei 430070, China; Chimie ParisTech, PSL University, CNRS, Institut de Recherche de Chimie Paris, 75005 Paris, France;* orcid.org/0000-0001-9018-7769

Xiujian Zhao − *State Key Laboratory of Silicate Materials for Architectures, Wuhan University of Technology, Hubei 430070, China;* orcid.org/0000-0002-2517-2605

Complete contact information is available at: https://pubs.acs.org/10.1021/jacs.9b12073

Notes

The authors declare no competing financial interest.

■ ACKNOWLEDGMENTS

This work was financially supported by the Natural Science Foundation of Hubei Province (2018CFA005), the Overseas Expertise Introduction Project (111 project) for Discipline Innovation of China (B18038), and the China Scholarship Council (201806950059). We acknowledge access to high-performance computing platforms provided by GENCI grant A0070807069.

■ REFERENCES

(1) Fan, F.; Voznyy, O.; Sabatini, R. P.; Bicanic, K. T.; Adachi, M. M.; McBride, J. R.; Reid, K. R.; Park, Y. S.; Li, X.; Jain, A.; Quintero-Bermudez, R.; Saravanapavanantham, M.; Liu, M.; Korkusinski, M.; Hawrylak, P.; Klimov, V. I.; Rosenthal, S. J.; Hoogland, S.; Sargent, E. H. Continuous-Wave Lasing in Colloidal Quantum Dot Solids Enabled by Facet-Selective Epitaxy. *Nature* **2017**, *544* (7648), 75−79.

(2) Yang, Y.; Zheng, Y.; Cao, W.; Titov, A.; Hyvonen, J.; Manders, J. R.; Xue, J.; Holloway, P. H.; Qian, L. High-Efficiency Light-Emitting Devices Based on Quantum Dots with Tailored Nanostructures. *Nat. Photonics* **2015**, *9* (4), 259−266.

(3) Wichner, S. M.; Mann, V. R.; Powers, A. S.; Segal, M. A.; Mir, M.; Bandaria, J. N.; DeWitt, M. A.; Darzacq, X.; Yildiz, A.; Cohen, B. E. Covalent Protein Labeling and Improved Single-Molecule Optical Properties of Aqueous CdSe/CdS Quantum Dots. *ACS Nano* **2017**, *11* (7), 6773−6781.

(4) Borrelli, N. F.; Smith, D. W. Quantum Confinement of PbS Microcrystals in Glass. *J. Non-Cryst. Solids* **1994**, *180*, 25−31.

(5) Han, K.; Im, W. B.; Heo, J.; Chung, W. J. A Complete Inorganic Colour Converter Based on Quantum-Dot-Embedded Silicate Glasses for White Light-Emitting-Diodes. *Chem. Commun.* **2016**, *52* (17), 3564−7.

(6) Ekimov, A. I.; Onushchenko, A. A. Quantum Size Effect in Three-Dimensional Microscopic Semiconductor Crystals. *JETP Lett.* **1981**, *34*, 345−348.

(7) Rossetti, R.; Nakahara, S.; Brus, L. E. Quantum Size Effects in The Redox Potentials, Resonance Raman Spectra, and Electronic Spectra of CdS Crystallites in Aqueous Solution. *J. Chem. Phys.* **1983**, *79* (2), 1086−1088.

(8) Han, K.; Yoon, S.; Chung, W. J. CdS and CdSe Quantum Dot-Embedded Silicate Glasses for LED Color Converter. *Int. J. Appl. Glass Sci.* **2015**, *6* (2), 103−108.

(9) Xia, M.; Liu, C.; Zhao, Z.; Wang, J.; Lin, C.; Xu, Y.; Heo, J.; Dai, S.; Han, J.; Zhao, X. Surface Passivation of CdSe Quantum Dots in All Inorganic Amorphous Solid by Forming Cd1-xZnxSe Shell. *Sci. Rep.* **2017**, *7*, 42359.

(10) Ohkubo, T.; Tsuchida, E.; Deguchi, K.; Ohki, S.; Shimizu, T.; Otomo, T.; Iwadate, Y. Insights from *Ab Initio* Molecular Dynamics Simulations for a Multicomponent Oxide Glass. *J. Am. Ceram. Soc.* **2018**, *101* (3), 1122−1134.

(11) Fossati, P. C. M.; Rushton, M. J. D.; Lee, W. E. Atomic-Scale Description of Interfaces in Rutile/Sodium Silicate Glass-Crystal Composites. *Phys. Chem. Chem. Phys.* **2018**, *20* (26), 17624−17636.

(12) Deng, L.; Du, J. Effects of System Size and Cooling Rate on the Structure and Properties of Sodium Borosilicate Glasses from Molecular Dynamics Simulations. *J. Chem. Phys.* **2018**, *148* (2), 024504.

(13) Konstantinou, K.; Sushko, P. V.; Duffy, D. M. Modelling the Local Atomic Structure of Molybdenum in Nuclear Waste Glasses with *Ab Initio* Molecular Dynamics Simulations. *Phys. Chem. Chem. Phys.* **2016**, *18* (37), 26125−26132.

(14) Konstantinou, K.; Duffy, D. M.; Shluger, A. L. Structure and Luminescence of Intrinsic Localized States in Sodium Silicate Glasses. *Phys. Rev. B: Condens. Matter Mater. Phys.* **2016**, *94* (17), 174202.

(15) Ishii, Y.; Salanne, M.; Charpentier, T.; Shiraki, K.; Kasahara, K.; Ohtori, N. A DFT-Based Aspherical Ion Model for Sodium

Aluminosilicate Glasses and Melts. *J. Phys. Chem. C* **2016**, *120* (42), 24370−24381.
(16) Pedone, A.; Malavasi, G.; Menziani, M. C.; Cormack, A. N.; Segre, U. A New Self-Consistent Empirical Interatomic Potential Model for Oxides, Silicates and Silica-Based Glasses. *J. Phys. Chem. B* **2006**, *110*, 11780−11795.
(17) Drijvers, E.; De Roo, J.; Martins, J. C.; Infante, I.; Hens, Z. Ligand Displacement Exposes Binding Site Heterogeneity on CdSe Nanocrystal Surfaces. *Chem. Mater.* **2018**, *30* (3), 1178−1186.
(18) Houtepen, A. J.; Hens, Z.; Owen, J. S.; Infante, I. On the Origin of Surface Traps in Colloidal II−VI Semiconductor Nanocrystals. *Chem. Mater.* **2017**, *29* (2), 752−761.
(19) Giansante, C.; Infante, I. Surface Traps in Colloidal Quantum Dots: A Combined Experimental and Theoretical Perspective. *J. Phys. Chem. Lett.* **2017**, *8* (20), 5209−5215.
(20) Del Ben, M.; Havenith, R. W. A.; Broer, R.; Stener, M. Density Functional Study on the Morphology and Photoabsorption of CdSe Nanoclusters. *J. Phys. Chem. C* **2011**, *115* (34), 16782−16796.
(21) Puzder, A.; Williamson, A. J.; Gygi, F.; Galli, G. Self-Healing of CdSe Nanocrystals: First-Principles Calculations. *Phys. Rev. Lett.* **2004**, *92* (21), 217401.
(22) Rabani, E. An Interatomic Pair Potential for Cadmium Selenide. *J. Chem. Phys.* **2002**, *116* (1), 258.
(23) Rabani, E. Structure and Electrostatic Properties of Passivated CdSe Nanocrystals. *J. Chem. Phys.* **2001**, *115* (3), 1493−1497.
(24) Smith, W.; Yong, C. W.; Rodger, P. M. DL_POLY: Application to Molecular Simulation. *Mol. Simul.* **2002**, *28* (5), 385−471.
(25) Ewald, P. P. Die Berechnung Optischer und Elektrostatischer Gitterpotentiale. *Ann. Phys.* **1921**, *369* (369), 253−287.
(26) Bussi, G.; Donadio, D.; Parrinello, M. Canonical Sampling through Velocity Rescaling. *J. Chem. Phys.* **2007**, *126* (1), 014101.
(27) Hoover, W. G. Canonical Dynamics: Equilibrium Phase-Space Distributions. *Phys. Rev. A: At., Mol., Opt. Phys.* **1985**, *31* (3), 1695−1697.
(28) Nosé, S. A Molecular Dynamics Method for Simulations in the Canonical Ensemble. *Mol. Phys.* **1984**, *52* (2), 255−268.
(29) Li, W.; Li, N.; Liu, C.; Greaves, G. N.; Ong, W. J.; Zhao, X. Understanding the Atomic and Electronic Structures Origin of Defect Luminescence of CdSe Quantum Dots in Glass Matrix. *J. Am. Ceram. Soc.* **2019**, *102* (9), 5375−5385.
(30) VandeVondele, J.; Krack, M.; Mohamed, F.; Parrinello, M.; Chassaing, T.; Hutter, J. Quickstep: Fast and Accurate Density Functional Calculations Using a Mixed Gaussian and Plane Waves Approach. *Comput. Phys. Commun.* **2005**, *167* (2), 103−128.
(31) Perdew, J. P.; Burke, K.; Ernzerhof, M. Generalized Gradient Approximation Made Simple. *Phys. Rev. Lett.* **1996**, *77* (18), 3865−3868.
(32) Goedecker, S.; Teter, M.; Hutter, J. Separable Dual-Space Gaussian Pseudopotentials. *Phys. Rev. B: Condens. Matter Mater. Phys.* **1996**, *54*, 1703−1710.
(33) VandeVondele, J.; Hutter, J. Gaussian Basis Sets for Accurate Calculations on Molecular Systems in Gas and Condensed Phases. *J. Chem. Phys.* **2007**, *127*, 114105.
(34) Demourgues, A.; Greaves, G. N.; Bilsborrow, R.; Baker, G.; Sery, A.; Speit, B. XAFS Study of CdSe Quantum Dots in a Silicate Glass. *Nucl. Instrum. Methods Phys. Res., Sect. B* **1995**, *97*, 166−168.
(35) Sun, J.; Zheng, X.; He, H.; Chen, X.; Dong, B.; Fei, R. Theoretical Study of Ligand and Solvent Effects on Optical Properties and Stabilities of CdSe Nanoclusters. *J. Mol. Struct.* **2016**, *1114*, 123−131.
(36) Wang, X.; Zeng, Q.; Shi, J.; Jiang, G.; Yang, M.; Liu, X.; Enright, G.; Yu, K. The Structure and Optical Absorption of Single Source Precursors for II-VI Quantum Dots. *Chem. Phys. Lett.* **2013**, *568*−*569*, 125−129.
(37) Xu, S.; Wang, C.; Cui, Y. Theoretical Investigation of CdSe Clusters: Influence of Solvent and Ligand on Nanocrystals. *J. Mol. Model.* **2010**, *16* (3), 469−73.
(38) Chung, S. Y.; Lee, S.; Liu, C.; Neuhauser, D. Structures and Electronic Spectra of CdSe-Cys Complexes: Density Functional Theory Study of a Simple Peptide-Coated Nanocluster. *J. Phys. Chem. B* **2009**, *113* (1), 292−301.
(39) Jose, R.; Zhanpeisov, N. U.; Fukumura, H.; Baba, Y.; Ishikawa, M. Structure-Property Correlation of CdSe Clusters Using Experimental Results and First-Principles DFT Calculations. *J. Am. Chem. Soc.* **2006**, *128*, 629−626.
(40) Hwang, Y.-N.; Shin, S.; Park, H. L.; Park, S.-H.; Kim, U. Effect of Lattice Contraction on the Raman Shifts of CdSe Quantum Dots in Glass Matrices. *Phys. Rev. B: Condens. Matter Mater. Phys.* **1996**, *54* (21), 15120−15124.
(41) Meulenberg, R. W.; Jennings, T.; Strouse, G. F. Compressive and Tensile Stress in Colloidal CdSe Semiconductor Quantum Dots. *Phys. Rev. B: Condens. Matter Mater. Phys.* **2004**, *70*, 235311.
(42) Ballauff, M.; Brader, J. M.; Egelhaaf, S. U.; Fuchs, M.; Horbach, J.; Koumakis, N.; Kruger, M.; Laurati, M.; Mutch, K. J.; Petekidis, G.; Siebenburger, M.; Voigtmann, T.; Zausch, J. Residual Stresses in Glasses. *Phys. Rev. Lett.* **2013**, *110* (21), 215701.
(43) Kurkjian, C. R.; Gupta, P. K.; Brow, R. K. The Strength of Silicate Glasses: What Do We Know, What Do We Need to Know? *Int. J. Appl. Glass Sci.* **2010**, *1* (1), 27−37.
(44) Mastelaro, V. R.; Zanotto, E. D. Residual Stresses in a Soda-Lime-Silica Glass-Ceramic. *J. Non-Cryst. Solids* **1996**, *194*, 297−304.
(45) Mu, L.; Feng, C. Topological Research on Lattice Energies for Inorganic Compounds. *MATCH Commun. Math. Comput. Chem.* **2006**, *56*, 97−111.
(46) Giberti, F.; Voros, M.; Galli, G. Design of Heterogeneous Chalcogenide Nanostructures with Pressure-Tunable Gaps and without Electronic Trap States. *Nano Lett.* **2017**, *17* (4), 2547−2553.

https://dx.doi.org/10.1021/jacs.9b12073
J. Am. Chem. Soc. 2020, 142, 3905−3912